

# A New Stator Back Iron Design For Brushless Doubly Fed Machines

Salman Abdi<sup>1</sup>, Ehsan Abdi<sup>2</sup>, *Senior Member, IEEE*, and Richard McMahon<sup>1</sup>

<sup>1</sup> Warwick Manufacturing Group (WMG), University of Warwick, Coventry, UK

<sup>2</sup> Wind Technologies Limited, St Johns Innovation Park, Cambridge, UK

Email: s.abdi.jalebi@gmail.com

**Abstract--** The brushless doubly-fed machine (BDFM) has been under investigation in its modern forms for 50 years. The reason for this interest is the machine's ability to operate as a brushless variable speed motor or generator through the use of a partially-rated power electronic converter connected to its second stator winding. Interest has increased in the last 20 years because of greater penetration of wind turbines with Doubly-Fed induction Generators (DFIGs) where brush gear and slip-ring maintenance and reliability have been a major issue. The BDFM appears in two forms, the brushless doubly fed induction machine (BDFIM), with two stator windings and a third closed rotor winding or the brushless doubly fed reluctance machine (BDFRM), with two stator windings and a reluctance rotor with no winding. This paper sets out to provide a rotor-centric view of BDFM operation, which shows the basis of its rotating flux pattern, aligning it with the known Natural Speed, and clarifying the synchronous and induction modes of operation of the BDFIM and the synchronous BDFRM. Based on rotor-centric view of the BDFM, it is shown that the conventional design methods for the BDFM stator back iron can be modified, leading to a lighter and smaller machine. The proposed design concepts are supported by analytical methods and their practicality is verified using 2-D Finite Element (FE) modeling and analysis of three experimental BDFMs.

**Index Terms--** brushless doubly-fed machine; brushless doubly-fed induction machine; brushless doubly-fed reluctance machine; electromagnetic theory; magneto-motive force; rotor winding; rotor reluctance; finite element analysis (FEA)

## I. INTRODUCTION

The Brushless Doubly-Fed Machine (BDFM) has been under development in its modern forms for nearly 50 years particularly in the UK, US, Brazil and China. The BDFM appears in two forms, both having two stator windings, the Brushless Doubly Fed Induction Machine (BDFIM), with two stator windings and a closed rotor winding, and the Brushless Doubly Fed Reluctance Machine (BDFRM), with two stator windings and a reluctance rotor with no winding.

Broadway et al. [1] analysed the BDFM from a stator winding magneto-motive force (MMF) point of view, following their pioneering work on the pole-amplitude modulated (PAM) Induction Motor. Wallace et al. [2] developed the first stator d-q axis analysis of the BDFM aimed at studying the machine's transient behaviour, for the purpose of controlling the Voltage-Source Converter

(VSC) connected to the BDFM's Control Winding. Williamson et al [3, 4] applied the machine air-gap MMF analysis, pioneered on the Induction Motor, to the BDFM in order to simplify operational understanding. A BDFM prototype was also constructed and finite element analysis of its magnetic field was performed. Roberts et al [5, 6] developed a mathematical theory for BDFM operation including an equivalent circuit, based on the Induction Motor, and showed that the equivalent circuit parameters can be extracted from cascade tests. McMahon et al [7, 8] used the equivalent circuit model to analyse BDFM practical aspects such as machine rating, stator core design, ride-through and rotor winding designs. A number of BDFMs ranging from 7-250 kW were constructed in collaboration with a spin-out company, Wind Technologies Ltd. A 20 kW BDFM wind turbine was successfully demonstrated [9] and a 250 kW BDFM in a D400 frame was built, see Fig. 1, demonstrating that large-scale BDFM is practical and constructible [10]. Runcos et al [11] in Brazil worked with WEG Industries and built prototype BDFMs up to 75 kW. Works in China have been spread amongst a number of universities working on both BDFIM and BDFRM design and control theory [12]. In addition, a number of experimental work has been performed in Netherland and Spain and reported for example in [13] and [14], mainly on BDFM design optimization and control strategies.

Almost all of the studies described above are based on stator-centric approach resulting in unified equivalent circuits to produce reliable predictions [6]. The stator-centric approach is necessary for studying the machine's performance because the rotor winding or reluctance structure is not easily accessible. However, it will be shown in this paper that previously proposed analytical calculation of the BDFM stator back iron based on stator-centric approach leads to overestimation of the back iron depth, because it was assumed that the BDFM stator back iron needs to be deep enough to carry two separate asynchronous magnetic fluxes. However, the resulting BDFM magnetic field pattern has no clear polar symmetry and the motion of the field is not a simple rotation. An alternative analytical method based on a rotor-centric approach is proposed for the stator back iron depth calculation and is validated by FE analysis, leading to an optimal value for the stator back iron depth.

## II. BACKGROUND THEORY

### A. Previous Studies on BDFM

The BDFM originated as a single-frame self-cascaded induction machine, in which two stator windings of different pole numbers share the same iron circuit with a rotor winding of related pole number [15]. The contemporary BDFM has two stator windings connected to different frequency supplies, producing different pole number magneto-motive forces (MMF) with no direct coupling between them, coupling being through the rotor only. The separate stator windings facilitate double feeding, with one winding connected to the grid called the power winding (PW) and the other via a partially rated power electronic converter called the control winding (CW), as shown in Fig. 2. The rotor winding carries an MMF induced by the stator windings and the rotor, and stator windings are coupled by the flux rotating in the common iron circuit.



Fig. 1. 250 kW D400 BDFIM (right front) on test bed.

The equivalent circuit for a BDFM, as shown in Fig. 3, was developed in [6] and improved in [7], the latter introducing the effects of stator and rotor core losses. The BDFIM flux is the resultant of three winding MMFs applied to the machine magnetic circuit. Based on Broadway et al's analysis [1] the BDFIM consists of:

- The stator power and control windings, with MMFs of differing pole pairs,  $p_1$  and  $p_2$ , fed at different angular frequencies,  $\omega_1$  and  $\omega_2$ ; PW and CW are designed for no direct coupling,  $p_1 \neq p_2$ , but coupled via the rotor only;
- Rotor Winding (RW),  $q$ -poles, fixed by the stator winding pole pair numbers,  $q=(p_1+p_2)$ , carrying an MMF induced by those stator windings;
- The PW, CW and RW MMFs act upon the machine air-gap to develop a flux, rotating in the machine's common iron magnetic circuit, coupling all those windings.

Williamson et al. [3] analysed the instantaneous BDFIM air-gap flux waves,  $b_{g1}$  and  $b_{g2}$  based upon the two stator windings as follows:

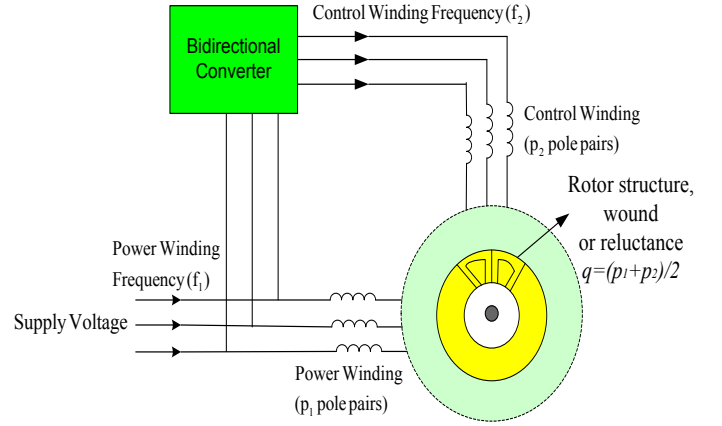


Fig. 2. Schematic of BDFM grid connection.

$$b_{g1}(\theta, t) = B_{g1} \cos(\omega_1 t - p_1 \theta - \alpha_1) \quad (1)$$

$$b_{g2}(\theta, t) = B_{g2} \cos(\omega_2 t - p_2 \theta - \alpha_2) \quad (2)$$

where  $\alpha_1$  and  $\alpha_2$  are the relative phases of the two flux waves and  $p_1$  and  $p_2$  are the PW and CW number of pole pairs. This reflects the total air-gap flux density but in terms of the two stator windings rather than the rotor side, thus perpetuating the concept of two machines in one frame. Williamson et al. also presented in [4] the first BDFM FE analysis and found out that the flux pattern has no clear polar symmetry and the motion of the field is not a matter of simple rotation and does not have a distinguishing N-S pattern. As a result, the conventional analytical method for determining depth of back iron used for an induction machine can not be utilised for the BDFM.

Roberts in [5] developed an analytical modeling for the BDFM rotor, which uses only a single d-q pair for each set of rotor circuits, while, the machine has two stator supplies of different pole numbers and as such, it is expected that two d-q pairs is required for each set of rotor circuits. This reinforces the fact that the BDFM performance is dominated with one flux system which is dedicated by its rotor structure complying with the rules mentioned in [5].

### B. Stator Back Iron Depth Calculation

The pole number and magnetic loading determine the back iron depth in conventional electrical machines. For the case of an induction machine, the stator back iron depth is calculated as:

$$y_c = \frac{\sqrt{2} B d}{2 p B_c} = \frac{\bar{B} \pi d}{4 p B_c} \quad (3)$$

where  $\bar{B}_c$  is the back iron maximum flux density,  $\bar{B}$  is the magnetic loading,  $p$  is the pole pair number, and  $d$  is the air gap diameter. However, the BDFM has a complex magnetic field pattern with no obvious polar symmetry and simple rotation. Using the BDFM stator-centric approach, McMahon et. al proposed an analytical method in [6] to calculate the stator back iron depth as:

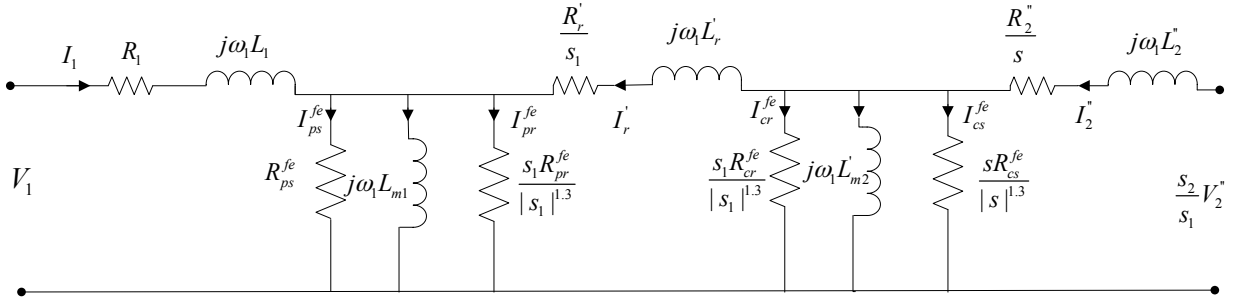


Fig. 3. Two terminal equivalent circuit of the BDFIM [11]

$$y_c = \frac{\sqrt{2}B_1 d}{2p_1 B_c} + \frac{\sqrt{2}B_2 d}{2p_2 B_c} = \frac{\sqrt{2}d}{2B_c} \left( \frac{B_1}{p_1} + \frac{B_2}{p_2} \right) \quad (4)$$

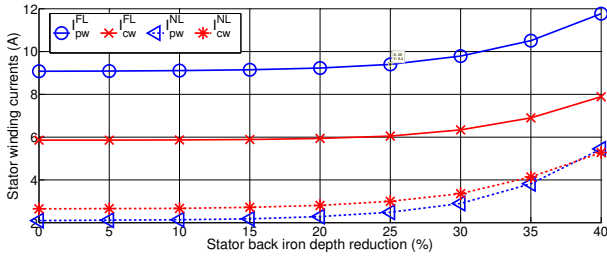


Fig. 4. Full-load ( $T \approx 100 \text{ N.m}$ ) and No-load ( $T \approx 0 \text{ N.m}$ ) stator PW and CW currents obtained for D180 BDFIM in synchronous mode of operation.

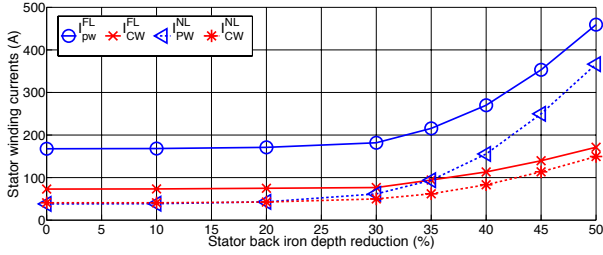


Fig. 5. Full-load ( $T \approx 3600 \text{ N.m}$ ) and No-load ( $T \approx 0 \text{ N.m}$ ) stator PW and CW currents obtained for D400 BDFIM in synchronous mode of operation.

where,  $B_1$  and  $B_2$  are the rms values of stator PW and CW flux densities. The FE analysis of prototype BDFMs performed in synchronous mode of operation shows that the stator back iron depth obtained from stator-centric approach is significantly larger than the required depth to avoid undesirable saturation. In order to investigate potential weight reduction in the stator back iron, the performance of two prototype BDFIMs with frame size D180 and D400 are analysed in their synchronous mode of operation when the stator back iron depth is reduced. The stator PW and CW currents in full-load and no-load conditions are shown in Figs. 4 and 5 for D180 and D400 BDFIMs, respectively. As it is obvious in Figs. 4 and 5, there are no significant increases in PW and CW currents in both full-load and no-load conditions when the stator back iron depth is reduced up to 30%. At this level of depth reduction, the maximum increase in a stator current from its rated value is below 3%. In the next section, an optimal design value for the BDFM stator back iron depth will be proposed based on a rotor-centric approach.

### III. BDFM ROTOR CENTRIC APPROACH

In this section the fundamental air gap MMF waves

are considered to find the total MMF acting across the air gap. It will then be shown that the response of the BDFM rotor winding structure to that MMF determines the field pattern in the machine's iron region. Hence, the fundamental flux wave of the BDFM, can be defined by the  $(p_1+p_2)$ -pole rotor design, linking stator and rotor iron, rather than the  $2p_1$  and  $2p_2$  poles stator windings.

The authors propose considering first the fundamental air-gap MMF waves i.e.  $\text{MMF}_{gs}$  due to the stator PW and CW, and  $\text{MMF}_{gr}$  due to the rotor winding reaction. Then considering the combined action of these MMFs summing to the total air gap MMF wave,  $\text{MMF}_g$ , which develops the machine magnetic field and therefore the rotor torque. Additional harmonics, due to the winding configuration add complexity but do not alter the fundamental result. On these bases, the stator MMF acting on the air gap can be given as:

$$\begin{aligned} \text{MMF}_{gs} = & k_{w1} N_1 I_1 \cos(\omega_1 t - p_1 \theta) \\ & + K_{w2} N_2 I_2 \cos(\omega_2 t - p_2 \theta - \lambda) \end{aligned} \quad (5)$$

Equation (5) can be resolved as:

$$\begin{aligned} \text{MMF}_{gs} = & 2k_{w1} N_1 I_1 \cos((\omega_1 + \omega_2)t / 2 + (p_1 + p_2)\theta / 2 - \gamma) \\ & \times \cos((\omega_1 - \omega_2)t / 2 + (p_1 - p_2)\theta / 2 + \gamma) \\ & - (k_{w2} N_2 I_2 - k_{w1} N_1 I_1) \cos(\omega_2 t - p_2 \theta - 2\gamma) \end{aligned} \quad (6)$$

The BDFM rotor winding must have  $q = p_1 \pm p_2$  poles to meet the BDFM rules [5]. The rotor structure with  $q = p_1 + p_2$  poles is popular, since it is difficult to achieve acceptable performance in a BDFM when a  $q = p_1 - p_2$  pole rotor is utilised.  $\text{MMF}_{gr}$  in this case is taken the form:

$$\begin{aligned} \text{MMF}_{gr} = & k_{wr} N_r I_r \{ \cos((\omega_1 + \omega_2)t / 2 \\ & + (p_1 + p_2)\theta / 2) \} \end{aligned} \quad (7)$$

It can be shown that for a BDFM to have reasonable PW and CW air gap magnetic fields, the stator windings are designed in a way to maintain the ratio of  $k_{w2} N_2 I_2 / k_{w1} N_1 I_1$  close to unity. In this case, in (6) the residual term (with the magnitude of  $k_{w2} N_2 I_2 - k_{w1} N_1 I_1$ ) is negligible compared to the main term and hence can be omitted from further analysis. Hence the stator MMF can be considered as two waves, one with  $p_1 + p_2$  pole pairs, and  $(\omega_1 + \omega_2) / (p_1 + p_2)$  rad/sec rotational speed, and another with  $p_1 - p_2$  pole pairs and  $(\omega_1 - \omega_2) / (p_1 - p_2)$  rad/sec rotational speed. For a BDFM with  $q = p_1 + p_2$  pole rotor design, the MMF reflected from the rotor is given by (7). With this

design therefore, the resulting MMF across the air gap will be:

$$\begin{aligned}
MMF_g &= MMF_{gs} - MMF_{gr} \\
&\approx 2k_{w1}N_1I_1 \cos\left((\omega_1 + \omega_2)t/2 + (p_1 + p_2)\theta/2 - \gamma\right) \\
&\quad \times \cos\left((\omega_1 - \omega_2)t/2 + (p_1 - p_2)\theta/2 + \gamma\right) \\
&- k_{wr}N_rI_r \left\{ \cos\left((\omega_1 + \omega_2)t/2 \right. \right. \\
&\quad \left. \left. + (p_1 + p_2)\theta/2 \right\} \right. \quad (8)
\end{aligned}$$

The result is that the rotor structure can only respond to one of the two fundamental components of the stator MMF wave (with  $(p_1 + p_2)/2$  pole pairs) and the rotor suppresses the other stator MMF wave (with  $(p_1 - p_2)/2$  pole pairs), resulting in end winding and air gap flux leakage. This ensures that the  $(p_1 - p_2)/2$  wave effectively appears in the leakage path only. Therefore, the fundamental flux wave of the BDFM, can be defined by the  $q$ -pole rotor design, linking stator and rotor, and rotating at  $(\omega_1 + \omega_2)/(p_1 + p_2)$ . This finding can be used to obtain an optimum design value for stator back iron depth if the BDFM is treated as a single-field induction machine with  $(p_1 + p_2)$  poles and the magnetic loading of  $\frac{2\sqrt{2}}{\pi} \sqrt{B_1^2 + B_2^2}$ . This is the BDFM magnetic loading, which is shown in [7] to be independent of the pole number combinations. The optimal value of the BDFM back iron depth can therefore be calculated using (3).

TABLE I  
A SUMMARY OF BDFM STATOR BACK IRON DEPTH CALCULATION METHODS STUDIED IN THIS PAPER

	Old Design	New Design
$y_c$ Term	$\frac{\sqrt{2}d}{2B_c} \left( \frac{B_1}{p_1} + \frac{B_2}{p_2} \right)$	$\frac{\bar{B}\pi d}{4pB_c}, p = p_1 + p_2$ $\bar{B} = \frac{2\sqrt{2}}{\pi} \sqrt{B_1^2 + B_2^2}$
$y_c$ Value	D180: 21.4 (mm) D400: 54.2 (mm)	14.5 (mm) 37.4 (mm)
Reduction in $y_c$	D180: – D400: –	32% 31%

This is summarised in Table I. The stator core back length in the new design method is about 32% and 31% smaller than in original design method in D180, and D400 BDFMs, respectively. This level of reduction has been shown in previous sections to be an acceptable limit before the machine is prone to saturation effects.

#### IV. EXPERIMENTAL VERIFICATION

Experimental verification for the proposed rotor-centric approach can be obtained from finite element analysis of magnetic flux for prototype BDFMs at different speeds and loads. In this paper, three prototype BDFMs with frame size D180 and D400 are being considered, their specifications are described in Table II.

The air gap scalar magnetic potentials,  $MMF_g(\theta)$ , have been extracted from FE analysis for prototype BDFMs and shown in Figs. 6 to 8 alongside their magnetic flux

plots. In addition, the air gap flux density of D400 BDFIM in synchronous mode of operation obtained from FE analysis and shown in Fig. 9.

TABLE II  
SUMMARY OF PROTOTYPE BDFMS USED IN FE ANALYSIS

BDFM Type	BDFIM	BDFRM	BDFIM
Reference	[7]	[10]	[11]
Year	2006	2011	2013
Frame Size	D180	D400	D400
Rating (kW)	22	250	250
$P_1$ PW Pole Pairs	2	3	2
$P_2$ CW Pole Pairs	4	2	4
$q$ poles	6	5	6
$N_s$ rev/min	500	600	500
Load Condition	Full load	Full load	No load
FE Plot Speed rev/min	834	1200	500

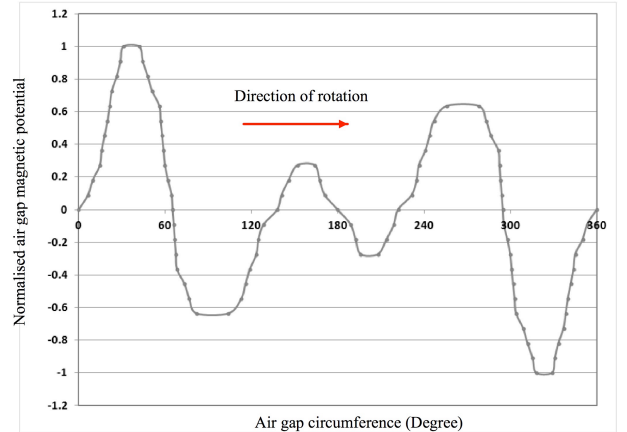
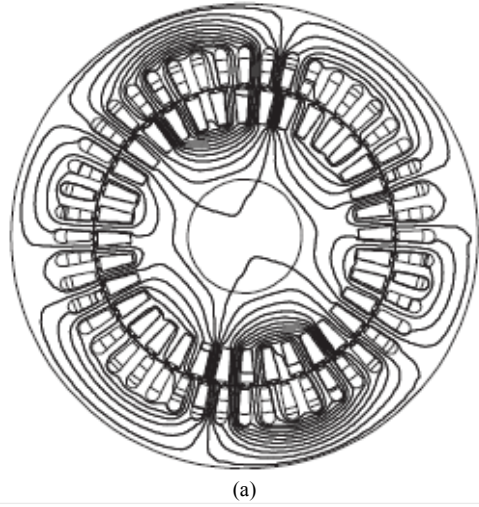


Fig. 6. 4/8 poles D180 BDFIM with 6-nest rotor (a) Finite element magnetic flux plot. (b) air gap scalar magnetic potential.

The normalised plots of scalar magnetic potential in all BDFMs show that the flux pulsates as it rotates. It can be also seen an obvious polar symmetry in these plots. The polarity of the plots is 6-pole for the 4/8 poles BDFIMs and 5-pole for 6/4 poles BDFRM, confirming the validity of  $q$ -pole rotor centric approach proposed in section III. The flux density plot for a 4/8 poles BDFIM shown in Fig. 9 also confirms the  $q$ -pole air gap flux density pattern of the BDFM demonstrating that the air gap flux density of a BDFM with  $p_1$  and  $p_2$  pole-pair

stator windings is similar to that of an induction machine with  $p_1+p_2$  pole pair, except that the flux pulsates as it rotates due to the effects of the two stator windings with different pole numbers and frequencies. The pulsation depends on the relative angular positions of the rotor elements in relation to the two stator windings.

It should be noted that although the flux plots are not purely sinusoidal, they show a near-sinusoidal air gap MMF pattern. The air gap flux form of a BDFM can be improved by better design of the rotor winding in the case of the BDFIM and reluctance structure in the case of the BDFRM [8].

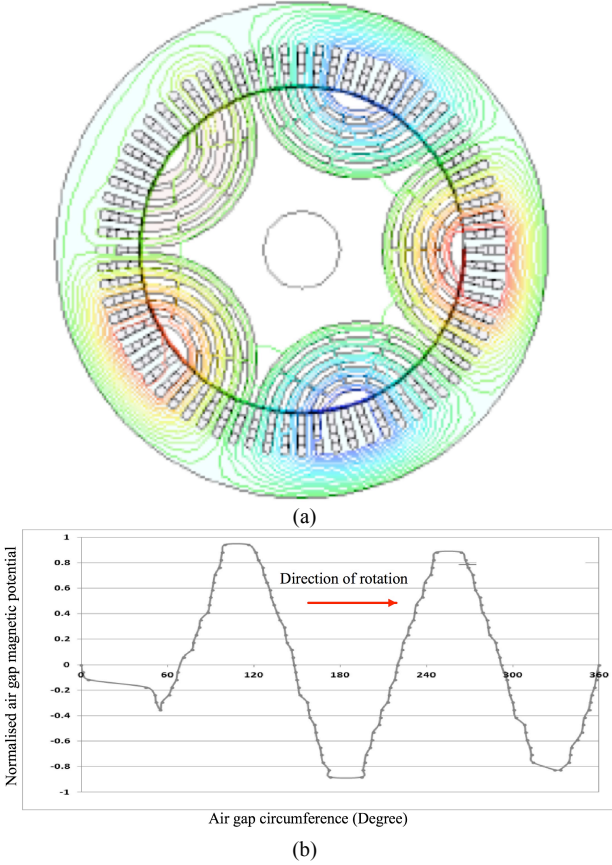


Fig. 7. 6/4 poles D400 BDFRM with 5-pole reluctance rotor (a) Finite element magnetic flux plot. (b) air gap scalar magnetic potential.

## V. CONCLUSION

This paper has demonstrated the following:

- The BDFM magnetic field, with stator windings of  $p_1$  and  $p_2$  pole pairs and a rotor winding structure of  $q=(p_1+p_2)$  elements, consists of a flux pattern coupling stator and rotor rotating at  $(\omega_1+\omega_2)/(p_1+p_2)$  rad/s. To date  $(p_1+p_2)$  rather than the  $(p_1-p_2)$  rotor elements have generally been selected for prototype BDFMs studied in published work, because of difficulties in achieving acceptable performance with  $q=(p_1-p_2)$ ;
- Since the BDFM rotor has by design a winding or reluctance structure of  $q=(p_1+p_2)$  elements or poles, the rotor has a flux pattern of  $q$ -poles rotating at  $\omega_r = (\omega_1+\omega_2)/q$  rad/s, with a Natural or Synchronous Speed of  $\omega_n = \omega_1/q$  rad/s. The rotor and stator

magnetic structures therefore need to be designed, for example in the terms of the back iron depth, to support a  $q$ -pole flux pattern rotating at  $\omega_r = (\omega_1+\omega_2)/q$  rad/s;

- The performance of the BDFM depends upon this single  $q$ -pole flux pattern. That performance also depends, in the case of a BDFIM, upon whether the rotor body is rotating synchronously or asynchronously with the  $\omega_r=(\omega_1+\omega_2)/q$  rad/s flux rotation, performing in synchronous or induction mode respectively. In the case of the BDFRM the rotor body will operate synchronously with that flux pattern and perform in synchronous mode;
- The air-gap flux density produced by the BDFM has been demonstrated from three prototype machines to be a  $q$ -pole wave, which is not a pure sinusoid just as the air-gap flux density of an IM, however, in the BDFM it pulsates as it rotates. This will be common to all BDFM machines, the non-sinusoidal air-gap flux wave and pulsation being the result of leakage flux harmonics due to combinations of the two stator winding and rotor element harmonics. The waveform of the air-gap flux density can be improved by the design of the rotor elements;
- The magnetic field in the BDFM can be characterized by a  $p_1 + p_2$  pole field rotating at  $(\omega_1 + \omega_2)/(p_1 + p_2)$  rad/sec. In order to determine the stator core back length, the BDFM can be considered as an induction machine with  $p_1+p_2$  poles and the magnetic loading of  $\frac{2\sqrt{2}}{\pi}\sqrt{B_1^2+B_2^2}$ . The FE

modeling has then been used to verify the proposed design methodology.

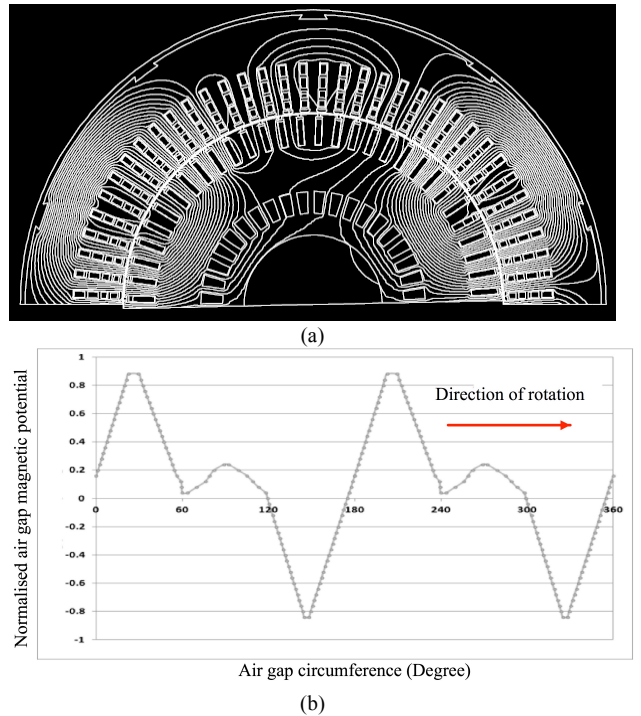


Fig. 8. 4/8 poles D400 BDFIM with 6-nest rotor (a) Finite element magnetic flux plot. (b) air gap scalar magnetic potential.

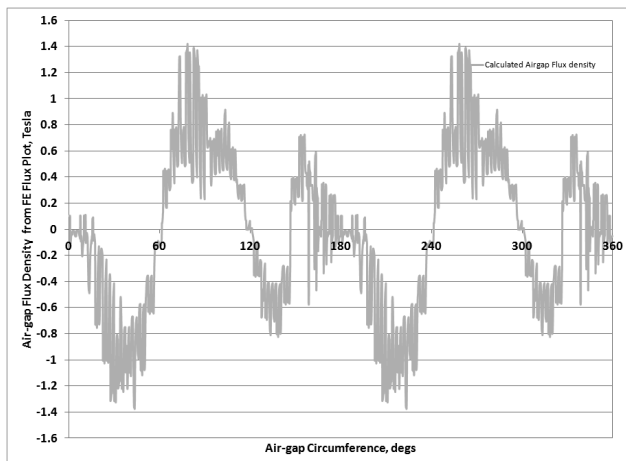


Fig. 9. D400 BDFIM air gap flux density obtained from FE analysis in synchronous mode of operation.

#### REFERENCES

- [1] A.R.W. Broadway, L. Burbridge, "Self-cascaded machine: a low-speed motor or high frequency brushless alternator", *Proc IEE*, 1970, 117, pp 1277–1290.
- [2] R. Li, A. Wallace, R. Spee, "Two-axis model development of cage-rotor brushless doubly-fed machines", *IEEE Trans Energy Convers*, 1991, 6, pp 453–460.
- [3] S. Williamson, A.C. Ferreira, and A.K. Wallace, "Generalized theory of the brushless doubly-fed machine Part I: Analysis", *IEE Proceedings - Electric Power Applications*, 1997, 144, (2), pp 111–122.
- [4] S. Williamson, A.C. Ferreira, "Generalised theory of the brushless doubly-fed machine. Part 2: model verification and performance", *IEE Proc, Electr Power Appl*, 1997, 144, pp. 123–129.
- [5] P.C. Roberts, "A Study of Brushless Doubly Fed (Induction) Machines", PhD dissertation, Emmanuel College, University of Cambridge, Cambridge, 2004.
- [6] P.C. Roberts, R.A. McMahon, P.J. Tavner, J.M. Maciejowski, and T.J. Flack, "Equivalent circuit for the brushless doubly fed machine (BDFM) including parameter estimation and experimental verification", *IEE Proceedings - Electric Power Applications*, 2005, 152, (4), pp 933–942.
- [7] R.A. McMahon, P.C. Roberts, X. Wang, and P.J. Tavner, "Performance of BDFM as generator and motor", *IEE Proceedings - Electric Power Applications*, 2006, 153, (2), pp 289–299.
- [8] R.A. McMahon, P.J. Tavner, E. Abdi, P. Malliband, D. Barker, "Characterizing brushless doubly-fed machine rotors", *IET Proceedings - Electric Power Applications*, 2013, In Press.
- [9] S. Shao, E. Abdi, R. McMahon, "Dynamic analysis of the brushless doubly fed induction generator during symmetrical three-phase voltage dips", *International Conference on Power Electronics and Drive Systems (PEDS)*, pp 464–469, Nov 2009, Taiwan.
- [10] E. Abdi, R. McMahon, P. Malliband, S. Shao, M. Matheka, P. Tavner, S. Abdi, A. Oraee, T. Long, and M. Tatlow, "Performance analysis and testing of a 250 kw medium-speed brushless doubly fed induction generator," *Renewable Power Generation, IET*, vol. 7, no. 6, pp. 631 – 638, 2013.
- [11] M. Ruviano, F. Rincos, N. Sadowski, I.M. Borges, "Analysis and test results of a brushless doubly fed induction machine with rotary transformer", *IEEE Trans Ind Electronics*, Vol. 59, No. 6, June 2012, 2670–2677.
- [12] H. Liu, L. Xu, "Performance analysis of a doubly excited brushless machine for variable speed application", *International conference on electrical machines and systems*, 2011, 1–4.
- [13] T. D. Strous, N. H. van der Blij, H. Polinder, and J. A. Ferreira, "Brushless doubly-fed induction machines: Magnetic field modelling," in *Int. Conf. Elect. Machines (ICEM)*, Sep. 2014, pp. 2702–2708.
- [14] J. Poza, E. Oyarbide, D. Roye, M. Rodriguez, "Unified reference frame dq model of the brushless doubly fed machine", *IEE Proceedings Electric Power Applications*, Vol. 53, Sep 2006, pp 726–734.
- [15] S. Abdi, E. Abdi, A. Oraee, R. McMahon, "Equivalent circuit parameters for large brushless doubly fed machines", *IEEE Transactions on Energy Conversion*, Vol. 29, No. 3, pp 706–715, April 2014.